

Simplified Three-dimensional Models for Studying the Non-uniformity inside the Flat-chip Solid Oxide Cell Stacks

Yingtian Chi^{1,4}, Yiwei Qiu¹, Jin Lin^{1,2*}, Qiang Hu², Yonghua Song³, Shujun Mu⁴

1 State Key Laboratory of Control and Simulation of Power Systems and Generation Equipment, Department of Electrical Engineering, Tsinghua University, Beijing 100087, China

2 Tsinghua-Sichuan Energy Internet Research Institute, Chengdu 610213, China

3 Department of Electrical and Computer Engineering, University of Macau, Macau 999078, China

4 National Institute of Clean-and-Low-Carbon Energy (NICE), Changping District, Beijing, 102211, China

ABSTRACT

This paper introduces the stacking scheme for the flat-chip solid oxide cells (FCSOCs). The FCSOCs are easy for manufacturing and stacking, combining the advantages of planar SOCs and tubular SOCs. The FCSOC stacks are sealed at the cold-ends (around 150°C) of single cells, enabling an easy, reliable, and flexible sealing with silicone sealants.

R&Ds reveal that, however, single cells in an FCSOC stack exhibit non-uniformity caused by the distribution of operating conditions. Fully-coupled 3D stack models validated with experiments are powerful tools for investigating the non-uniformity, which, however, require high computation costs, especially for large stacks with up to about 100 cells. Inspired by that the stack model's focus is the stack-level non-uniformity but not the cell-level non-uniformity, it is possible to simplify the fully-coupled model by ignoring cell-level non-uniformity. Therefore, a data-driven method, called the adaptive polynomial approximation (APA), is used to build surrogate models of single cells. The cell-level surrogate models are then integrated into the stack-level model to form a hybrid model that avoids computing the current distribution and fuel-side mass distribution inside the single cells. The computational cost is reduced, making it possible to simulate the models of large stacks. The simplification error is analyzed. Based on the simplified stack models, the design and operation factors inducing the non-uniformity among single cells are investigated and optimized.

Keywords: Flat-chip solid oxide cell stack, 3D models, simplification, non-uniformity, multi-scale, hybrid model

NONMENCLATURE

Abbreviations

APA Adaptive polynomial approximation
FCSOC Flat-chip solid oxide cell

Symbols

T_{av} Average temperature of the outer electrode of a single cell
 I Current
 FU Fuel utilization of a single cell
 $p_{O_2,av}$ Average oxygen partial pressure on the outer electrode of a single cell
 Q_{H_2} Flow rate of hydrogen
 Q_{air} Flow rate of air
 V_{cell} Cell voltage
 Q_{heat} Total electrochemical heat source of a single cell
 Q_{mass,O_2} Total oxygen mass source (i.e., consuming rate) of a single cell due the electrochemical reaction

1. INTRODUCTION

Planar SOCs (PSOCs) and tubular SOCs (TSOCs) are two prevalent structures of SOCs. PSOCs have the advantages of easy manufacturing and large power density, but the sealing of PSOCs is troublesome due to the high temperature and the thermal expansion mismatch among ceramic and metallic materials [1,2]. TSOCs are robust and easy for sealing but are limited by the power density as well as fabrication method [3,4]. Flat-tubular

SOCs (FTSOCs) have been proposed to combine the PSOCs' merit of large power density and TSOCs' merit of easy sealing, making FTSOCs a popular structure [5-7]. However, most FTSOCs are fabricated via extrusion, which limits the low-cost mass production.

In [8], our group proposed the flat-chip SOC (FCSOCs) manufactured via tape casting and screen printing which are mature technologies applied for the production of PSOCs, enabling low-cost production. The FCSOCs are robust to thermal cycles and thermal shocks, improving the SOC system's reliability. The first generation of FCSOC is electrolyte-supported, resulting in a low power density and a working temperature of around 800°C. In [9], we reported the latest anode-supported generation of FCSOC, lowering the working temperature to 600°C and improving the power density. In this paper, the stacking scheme for the anode-supported FCSOCs is introduced for the first time. The sealing for the stack is conducted at the cold-ends of cells (around 150°C), enabling silicone sealants to be used for a convenient, reliable, and flexible sealing. Stacks composed of different numbers of single cells have been designed and assembled.

During R&D, however, it is found that single cells inside a stack exhibit non-uniform performances caused by the non-uniform distribution of operating conditions. To investigate the non-uniformity's reasons and effects, a 3D fully-coupled stack model is built for a seven-cell short stack and validated with the experiment data. However, the fully-coupled models simulate the multi-

scale transfer phenomena from micrometer-scale to meter-scale, whose high computational cost limits their application to larger stacks containing up to 100 cells. In the literature, several simplification approaches have been proposed to improve the computational efficiency of 3D PSOC stack models. Banerjee et al. [10] proposed a hierarchical modeling approach that used a simplified 2D repeating unit model and selected the representative repeating units to form the 3D stack model. Navasa et al. [11] and Miao et al. [12] approximated the fine channel and PEN structures with a homogenized volume, which reduced the mesh elements and accelerated the computation by two orders of magnitude. Ba et al. [13] used artificial neural networks (ANNs) to build surrogate models for unit cells which were integrated into the 3D stack model to avoid calculating the electrochemistry and improve computational efficiency.

Nonetheless, these simplification approaches for PSOC stack models can hardly be directly applied to FCSOC stack models due to the FCSOC's unique geometry. To fill in this gap, this paper proposes to use a data-driven method, called the adaptive polynomial approximation (APA), to build surrogate models of single cells, and integrate the cell-level surrogate models into the stack-level model that only simulates the heat transfer and air-side mass transfer. Therefore, the computation of fuel-side mass transfer and cell-level charge transfer is eliminated, which alleviates the computational burden. Additionally, the surrogate models are polynomials and can be readily integrated into stack-level models built with commercial CFD

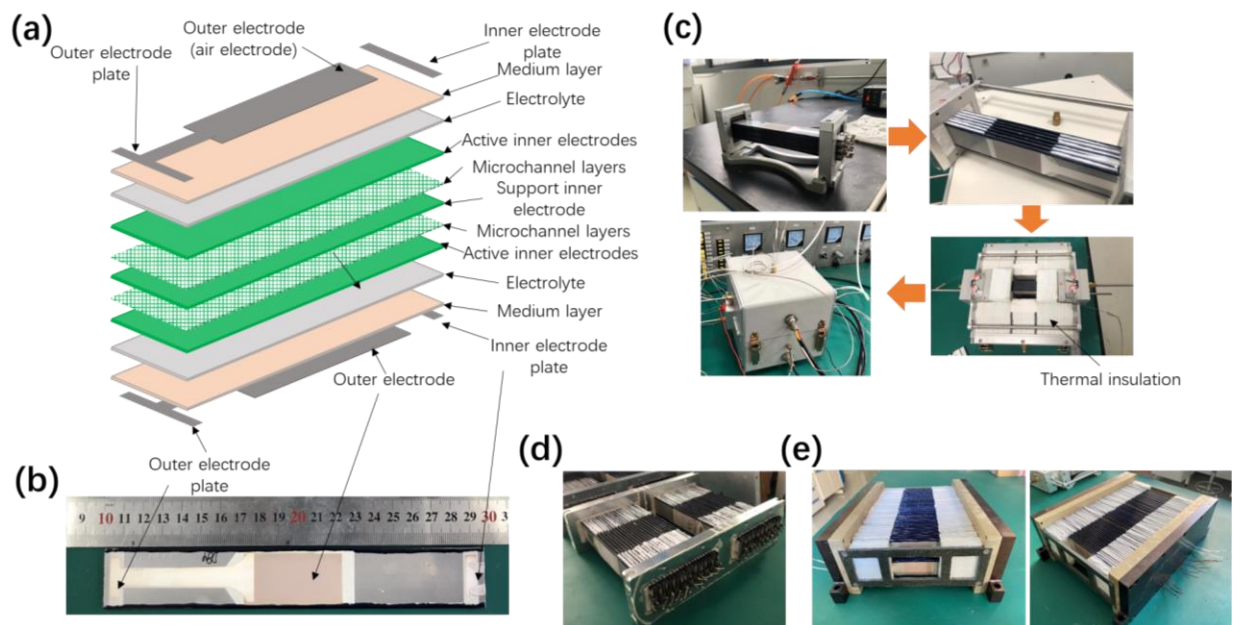


Fig. 1. (a) Structure of a FCSOC Cell. (b) A real FCSOC single cell. (c) Assembling process of a seven-cell FCSOC short stack. (d) Stack composed of 60 cells. (e) Stack composed of 120 cells (arranged in two rows).

software, requiring only slight modification of the fully-coupled models.

In this paper, the improved computational efficiency of the simplification method is illustrated, and the simplification error is evaluated. Based on the simplified models, the design and operation factors affecting the non-uniformity are discussed.

2. METHODS

2.1 Flat-chip SOCs and Stacks

The FCSOC single cell and stack are introduced first. Fig.1 (a) and (b) show the structure of an FCSOC and a real FCSOC. The FCSOC has a symmetrical structure manufactured via tape-casting and screen-printing, making low-cost, large-scale production possible. The fuel (inner) electrode and the air (outer) electrode are located inside the cell and on the outside surface of the cell, respectively. There are micro-channels inside the inner electrode, allowing gas to pass through. Current collecting is implemented by attaching conductive wires to the inner and outer electrode plates. Fig.1 (c) demonstrates the assembling process of a short stack containing seven cells. Both ends of the single cells are first inserted into the frames, and the gaps between cells and frames are sealed. Then, the fuel-side chamber is assembled onto the frames, while the silver wires connected to electrode plates are extracted through the holes on the chamber's wall. The stack is put into the heat-insulation shell, inside which there is an air chamber with heating cords installed on its inner surface. In this design, only the center of the stack is under high temperature, and the sealing is conducted on the cold ends of the cells with silicone sealants, called cold-end sealing. This design enables convenient, flexible, and reliable sealing and stacking. Various sizes of stacks have been developed. Fig.1 (d) shows a stack containing 60 cells, while Fig.1 (e) shows a larger stack composed of 120 cells, which are arranged in two rows.

2.2 Fully-coupled 3D Models and the Simplification Method based on APA

One of the R&D's focuses has been put to optimize the stack's structure and operating conditions to improve the uniformity among cells. For this purpose, fully-coupled stack models are built. Fig.2 (a) shows the model geometry of a seven-cell short stack model developed according to the real stack in Fig.1 (c). The model is symmetrical, and therefore only half of a real stack is modeled. The model includes electrochemistry, heat transfer, mass transfer, and charge transfer. For brevity,

the model's detail is not described here as there are various similar SOC models in existing literature (e.g., [14]), and the fully-coupled one in this paper has no apparent difference except the geometry. Fig.2 (b) compares the simulated and measured IV curves under different temperatures and Q_{air} (the fuel-side is pure hydrogen with a flow rate of 150sccm), indicating a good match between model simulation and experiments. Due to the fully-coupled physics, the seven-cell stack model takes a long time and large memory for computing even a single stationary condition, hindering the simulation for large stacks like those in Fig.1 (d) and (e).

To reduce the computational cost, a simplification method is proposed, illustrated in Fig.2 (c). The inspiration is that the focus of the stack model is the non-uniformity among different cells, the key factor affecting stack performances, but not the non-uniformity on a single cell. The latter is, however, computed by the fully-coupled model, including the distribution of current, mass, and heat source. Therefore, a simplification approach is proposed as follows.

In the fully-coupled model, the cell-level fine model is coupled with the stack-level model by providing the

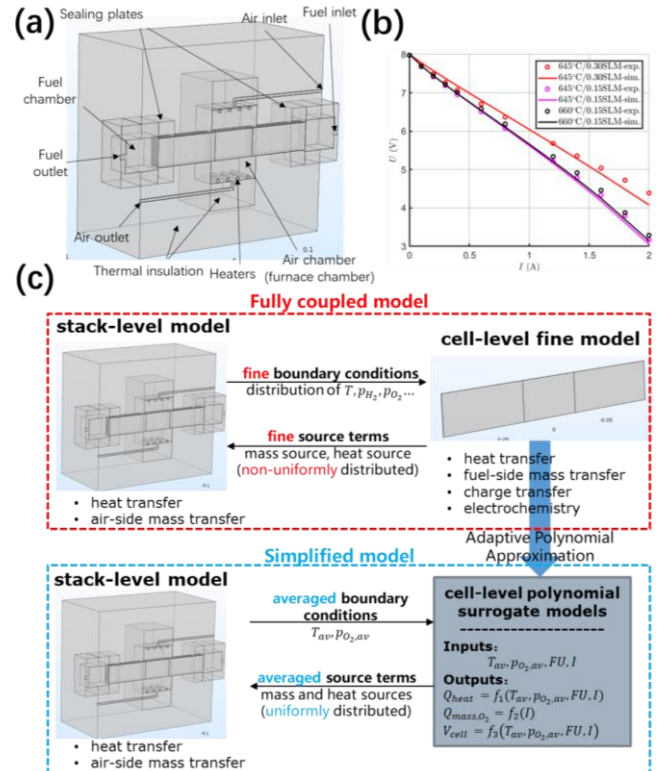


Fig. 2. (a) Structure of a seven-cell short stack model. (b) Validation under different temperature and Q_{air} . (c) Illustration of the simplification method.

electrochemical heat source term and mass source terms of O_2 , H_2 , and H_2O , while the stack-level model provides

the distribution of $T, p_{O_2}, p_{H_2}, p_{H_2O}$ as the boundary conditions for cell-level models. To avoid computing the cell-level non-uniform distributions of mass and heat sources which do not significantly affect the stack-level temperature and mass distributions, the APA data-driven method, proposed by our group in [9], is used to build surrogate models for single cells. In other words, the cell-level fine model is simulated under several sampling points (different values of $T_{av}, I, FU, p_{O_2,av}$), and the simulation results are used to identify the relationships between $Q_{heat}, Q_{mass,O_2}, V_{cell}$ and $T_{av}, I, FU, p_{O_2,av}$, formulated as follows.

$$Q_{heat} = f_1(T_{av}, I, FU, p_{O_2,av})$$

$$= a_{1,0} + a_{1,1}T_{av} + a_{1,2}I + a_{1,3}FU + a_{1,4}p_{O_2,av} + \dots$$

$$Q_{mass,O_2} = f_2(I) = M_{O_2}I/4F$$

$$V_{cell} = f_3(T_{av}, I, FU, p_{O_2,av})$$

$$= a_{3,0} + a_{3,1}T_{av} + a_{3,2}I + a_{3,3}FU + a_{3,4}p_{O_2,av} + \dots$$

$a_{i,j}$ is the coefficient of the j th term in the i th model. The number of terms and the values of $a_{i,j}$ are adaptively determined by the APA method, whose detail is described in [9]. Q_{mass,O_2} is directly calculated by the current I since I represents the electrochemical reaction rate. M_{O_2} is O_2 's molar mass, and F is the Faraday constant. The units of $Q_{heat}, Q_{mass,O_2}, V_{cell}$ are W, kg/s, and V.

In the simplified model, T_{av} and $p_{O_2,av}$ are calculated by the stack-level model and passed to the cell-level surrogate models, while I and FU are directly specified. Then, the cell-level surrogate models of Q_{heat} and Q_{mass,O_2} are used to calculate the average volumetric heat source and the surface mass source, which is integrated into the stack-level model. The cell voltages are calculated using the surrogate model of V_{cell} . In this way, the simplified model ignores non-uniformity on a single cell while it keeps the non-uniformity among different cells. Therefore, the computational efficiency is improved.

Additionally, the surrogate models are polynomials that can be conveniently integrated into commercial CFD software like COMSOL with only slight modifications of the original fully-coupled model. Delicately designed computational code and modification of the material properties and governing equations that are needed in [10-12] are not required in this paper.

3. RESULTS AND DISCUSSION

3.1 Effects of Simplification

With the help of the APA method, the surrogate models are built with low sampling cost. 903 sampling points are used for the surrogate models of V_{cell} and Q_{heat} to reach the accuracy of 2mV and 5mW. For comparison, 10000 sampling points are used in [13] to train the ANN surrogate models that also have four inputs.

To illustrate the accuracy of simplification, Fig. 3 (a)-(d) compares the $V_{cell}, T_{av}, p_{O_2,av}$ and FU simulated by the fully-coupled and simplified seven-cell stack model. Q_{air} , the overall hydrogen utilization and the

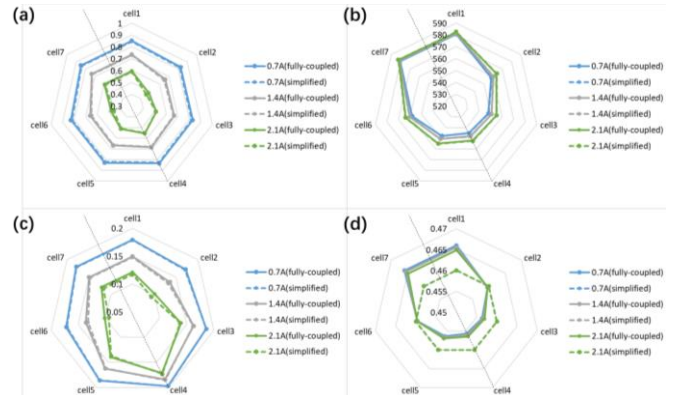


Fig. 3. Comparisons of the distributions of (a) V_{cell} / V , (b) $T_{av} / ^\circ C$, (c) $p_{O_2,av} / 1$ and (d) $FU / 1$ simulated by the fully-coupled models and simplified models.

stack temperature set-point are set to 800sccm, 46%, and 600°C, while I varies from 0.7A to 2.1A. The dashed lines represent the symmetrical axis (i.e., cell 4 is the cell in the middle of the stack, while cells 1 and 7 are the cells on the two sides of the stack). Fig. 3 (a) shows that the simplified model accurately approximates the non-uniform distribution of V_{cell} , while the approximation error slightly increases when I increases, especially for cells 2 and 6. T_{av} is approximated accurately under all cases indicated by Fig. 3 (b), while Fig. 3 (c) reveals that the approximation error of $p_{O_2,av}$ becomes larger for cells 2 and 6 as I increases. Fig.3 (d) reflects the distribution of hydrogen flow rates among cells. The simplified model assumes a uniform distribution of hydrogen flow, which has small errors for cells 1,3,4,5, and 7. According to Fig. 3, it is therefore concluded that the approximation error of V_{cell} originates from the error in $p_{O_2,av}$.

Fig. 4 (a) compares the computational cost of simplified models and fully-coupled models. To eliminate

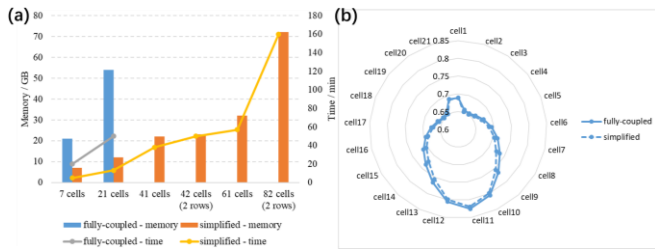


Fig. 4. (a) Comparisons of computational time and memory of fully-coupled and simplified models. (b) Comparisons of the distributions of V_{cell} [V] simulated by the fully-coupled models and simplified models.

the influence of mesh, the same mesh is applied for the simplified model and the fully-coupled model of the same stack, and similar mesh sizes are used for different stacks. Simulations are executed on a computer with 128GB memory and 36 cores. Due to the limited memory, fully-coupled models of seven-cell and 21-cell stacks are simulated. The results show that the simplification method significantly reduces the required memory and time by about 75%, mainly attributed to the ignored fuel-side mass transfer, and therefore enables the simulation of large stacks. Fig.4 (b) shows the simulated cell voltage distribution of a 21-cell stack (symmetrical). Q_{air} , I , the overall hydrogen utilization and the stack temperature set-point are set to 1000sccm, 1A, 49%, and 630°C. The good match between the result of the fully-coupled models and that of the simplified model validates the simplification method's applicability for larger stacks.

3.2 Factors influence the non-uniformity

The simplified model is used to study the influence of operating parameters and design on the non-uniformity of a 21-cell stack. A non-uniformity index, called the coefficient of variation (CV), is used to quantify the non-uniformity of cell voltages. $V_{cell,i}$ is the voltage of the i th cell. N_{cell} is the number of cells. A larger CV indicates a more non-uniform distribution of cell voltages.

$$CV = \left(\frac{1}{N_{cell}} \sum_{i=1}^{N_{cell}} \left(\frac{V_{cell,i} - \sum_{i=1}^{N_{cell}} V_{cell,i} / N_{cell}}{\sum_{i=1}^{N_{cell}} V_{cell,i} / N_{cell}} \right)^2 \right)^{0.5}$$

Fig. 5(a) shows how the non-uniformity is affected by different operating parameters. 'original' refers to the original stack design with only one air inlet and one air outlet as shown in Fig. 2(a), while 'modified' refers to the modified design shown in Fig. 5(b) with multiple air inlets and outlets. The influences of FU , I , T and Q_{air} are studied. For comparisons, the operating parameters are normalized as follows.

$[\cdot]_{normalized} = ([\cdot] - [\cdot]_{min}) / ([\cdot]_{max} - [\cdot]_{min})$
 $[\cdot]$ represents FU, I, T or Q_{air} . $[\cdot]_{max}$ is 0.75, 2.2A, 650°C, and 2200sccm, and $[\cdot]_{min}$ is 0.15, 0.2A, 550°C, and 800sccm, respectively. When one of the operating parameters is varied, the others are fixed at 0.5 (normalized). In Fig.5 (a), the results of the original design (solid lines) show that the non-uniformity significantly increases with I . A possible reason is a non-uniform distribution of p_{O_2} , caused by the non-uniform distribution of airflow. Therefore, the modified design in Fig.5 (b) increases the number of air inlets and outlets in order to obtain a more uniform airflow distribution. Fig. 5(c) and Fig. 5(d) compare the simulated p_{O_2} distributions of the original design and the modified design under the same operating condition, indicating that the modified design effectively improves the uniformity of airflow distribution. Besides, Fig. 5(a) also shows the results of the modified design (dashed lines), which demonstrates that the modified design effectively improves the uniformity of cell voltages by over 50%.

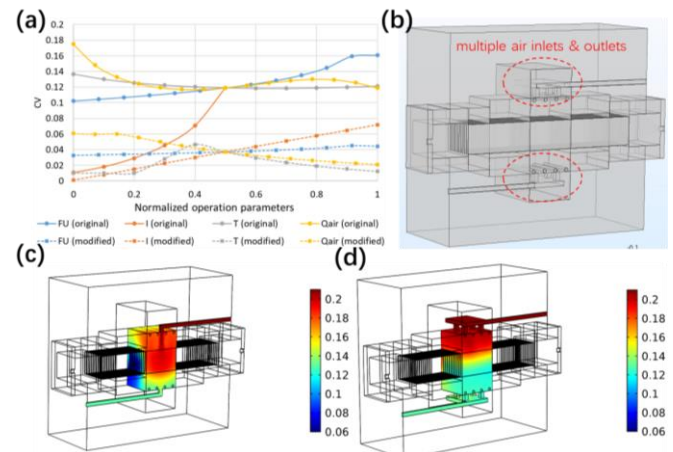


Fig. 5. (a) Non-uniformity of cell voltages under different operating conditions. (b) Modified stack design with multiple air inlets and outlets. p_{O_2} distributions of the (c) original and (d) modified stack design.

4. CONCLUSION

This paper introduces a flexible stack scheme for FCSOCs and a data-driven hybrid simplification method for reducing the computational cost of the 3D FCSOC stack models. The simplification is achieved by integrating data-driven cell-level surrogate models into stack-level 3D physical models so that the unnecessary calculation of current distribution and fuel-side mass distribution of the fully-coupled 3D physical models are eliminated. The simplification method provides a way to decouple the large-scale model with the small-scale

model when the small-scale fine distribution does not influence the large-scale performance.

Comparisons with the fully-coupled model show that the simplified model retains accuracy while it reduces the computational cost by about 75%, making it practical to simulate the models of stacks with up to 100 cells, which is indispensable for future R&D.

The simplified model is used for studying the performance non-uniformity of stacks. The influence of operating parameters is studied. It is found that the non-uniform distributed airflow is one origin of the voltage non-uniformity. Therefore, a modified design with multiple air inlets and outlets is proposed, which improves the uniformity by over 50%.

Future R&D will focus on improving the power density of the FCSOC stack, as well as building faster steady-state and dynamic models in order to support the R&D process.

ACKNOWLEDGEMENT

This work was supported by the Chinese National Key Research and Development Program (2018YFE0106700).

REFERENCE

[1] S. Lee, Y. hoon Jang, H. Y. Shin, K. Lee, M. Bae, J. Kang, J. Bae, Reliable sealing design of metal-based solid oxide fuel cell stacks for transportation applications, *International Journal of Hydrogen Energy* 44 (2019) 30280–30292.

[2] S. Bremm, S. Dölling, W. Becker, L. Blum, R. Peters, J. Malzbender, D. Stolten, A methodological contribution to failure prediction of glass ceramics sealings in high-temperature solid oxide fuel cell stacks, *Journal of Power Sources* 507 (2021) 230301.

[3] T.-H. Lim, J.-L. Park, S.-B. Lee, S.-J. Park, R.-H. Song, D.-R. Shin, Fabrication and operation of a 1 kw class anode-supported flat tubular sofc stack, *International Journal of Hydrogen Energy* 35 (2010) 9687–9692.

[4] H. Zeng, S. Gong, Y. Wang, Y. Shi, Q. Hu, N. Cai, Flat-chip flame fuel cell operated on a catalytically enhanced porous media combustor, *Energy Conversion and Management* 196 (2019) 443–452.

[5] K. Rashid, S. K. Dong, R. A. Khan, S. H. Park, Optimization of manifold design for 1 kw-class flat-tubular solid oxide fuel cell stack operating on reformed natural gas, *Journal of Power Sources* 327 (2016) 638–652.

[6] S. Park, N. M. Sammes, K.-H. Song, T. Kim, J.-S. Chung, Monolithic flat tubular types of solid oxide fuel cells with integrated electrode and gas channels, *International Journal of Hydrogen Energy* 42 (2017) 1154–1160.

[7] W. Liu, Z. Zou, F. Miao, X. Li, J. Wang, J. Yang, J. Wilson, X. Zhou, Z. Zhong, Q. Zhai, W. Guan, Anode-supported planar solid oxide fuel cells based on double-sided cathodes, *Energy Technology* 7 (2019) 240–244.

[8] S. Gong, H. Zeng, J. Lin, Y. Shi, Q. Hu, N. Cai, A robust flat-chip solid oxide fuel cell coupled with catalytic partial oxidation of methane, *Journal of Power Sources* 402 (2018) 124–132.

[9] Y. Chi, Y. Qiu, J. Lin, Y. Song, W. Li, Q. Hu, S. Mu, M. Liu, A robust surrogate model of a solid oxide cell based on an adaptive polynomial approximation method, *International Journal of Hydrogen Energy* 45 (2020) 32949–32971.

[10] A. Banerjee, Y. Wang, J. Diercks, O. Deutschmann, Hierarchical modeling of solid oxide cells and stacks producing syngas via h₂o/co₂ co-electrolysis for industrial applications, *Applied Energy* 230 (2018) 996–1013

[11] M. Navasa, X.-Y. Miao, H. L. Frandsen, A fully-homogenized multiphysics model for a reversible solid oxide cell stack, *International Journal of Hydrogen Energy* 44 (2019) 23330–23347.

[12] X.-Y. Miao, O. B. Rizvandi, M. Navasa, H. L. Frandsen, Modelling of local mechanical failures in solid oxide cell stacks, *Applied Energy* 293 (2021) 116901.

[13] L. Ba, X. Xiong, Z. Yang, Z. Lei, B. Ge, S. Peng, A novel multi-physics and multi-dimensional model for solid oxide fuel cell stacks based on alternative mapping of bp neural networks, *Journal of Power Sources* 500 (2021) 229784.

[14] A. Li, C. Song, Z. Lin, A multiphysics fully coupled modeling tool for the design and operation analysis of planar solid oxide fuel cell stacks, *Applied Energy* 190 (2017) 1234–1244.